density at that wavelength, $OD_{65\,nm} = 0.035$, between 0.17 and 10.5 ps after excitation must be due *only* to the formation of HOCD. For the concomitant disappearance of the precursor BR, the equivalent maximum contribution to spectral change can then be estimated at $|\Delta OD| \leq 0.0017$, which is below the noise level of our transient spectra. To summarize so far:

First, the transient spectrum a of Figure 2 originates mainly from a product state of internal relaxation within the aromatic endoperoxide. This product state is populated ultrafast, i.e., even during the pump pulse of 0.26 ps; then its population does not change appreciately on a 100-ps time scale. We speculate that this product state is $S_2(n\pi^*)$-excited HOCDPO.

Second, the evolution toward spectrum b and associated with a time constant of 1.6 ps is due only to the formation of HOCD.

A third time constant, of ca. 5 ps, was found for a gradual decrease in absorbance at 450 nm. Similarly, a decrease of absorbance at the red side of the main HOCD absorption band was observed (cf. Figure 2b,c). Both may be explained as a result of cooling of the HOCDPO product state and of hot ground-state HOCD, respectively.

Finally, consider the large variation of rise times τ_2, in the range 1.6-75 ps, for the photocycloreversion of endoperoxides.[6-10] It was recently shown by Jesse et al.[10] for the endoperoxide of heterocoerdianthrone (HECDPO) that the development of HECD is a thermally activated process, with activation energy $E_a = 5.7$ kcal/mol. The very large preexponential factor, $A = 10^{14.8}$ s^{-1}, points to the allowedness of the thermal reaction, which at 22 °C has $\tau_2 = 40$ (±10) ps. With regard to the present case of HOCDPO, assuming the same preexponential factor but an activation energy that is lower by 1.9 kcal/mol would account for the 25-fold shorter rise time $\tau_2 = 1.6$ ps. Thus the apparent large variation of experimentally found τ_2 values could be reduced to a relatively small change in energy barrier for an activation-controlled process.

Conclusion

Using HOCDPO as model compound, the photocycloreversion of an aromatic endoperoxide to its aromatic parent has been followed for the first time by transient absorption spectroscopy in the subpicosecond to 10-ps time range. Only two contributing transient spectra are distinguished: that of a primary product state for internal relaxation of the aromatic endoperoxide—most likely $S_2(n\pi^*)$-excited HOCDPO—and that of the hot product HOCD. The observations are consistent with the current two-step model for the reaction. HOCD is produced in the ground state in a thermal, secondary reaction. Its biradical precursor does not contribute significantly to transient optical absorption in the visible spectral range. The lifetime of the biradical is inferred from the rise time of HOCD absorption to be 1.6 ps.

Acknowledgment. We are grateful to Prof. F. P. Schäfer for a critical reading of the manuscript and to the Deutsche Forschungsgemeinschaft for support through the Leibniz Prize Program.

A Kinetic Investigation of the Ca/CaO System: Non-Arrhenius Behavior of the Reaction $Ca(^1S) + N_2O$ over the Temperature Range 250-898 K and a Study of the Reaction CaO + O

John M. C. Plane* and Chia-Fu Nien

Rosenstiel School of Marine and Atmospheric Science and the Department of Chemistry, University of Miami, Miami, Florida 33149 *(Received: November 17, 1989; In Final Form: February 5, 1990)*

A study is presented of the reaction $Ca(^1S) + N_2O$ over the temperature range 250-898 K. Ca atoms were produced in an excess of N_2O and He bath gas by the pulsed two-photon (193.3 nm) dissociation of CaI_2 and then monitored by time-resolved laser-induced fluorescence spectroscopy at $\lambda = 422.7$ nm ($Ca(4^1P_1-4^1S)$). Above 500 K there is a clear upward curvature in the Arrhenius plot, and the best description of the temperature dependence of the rate constant over the experimental temperature range is given by $k(T) = (2.43 \pm 0.29) \times 10^{-11} \exp[-(6.84 \pm 0.27)\ \text{kJ mol}^{-1}/RT] + (9.70 \pm 1.39) \times 10^{-10} \exp[-(24.58 \pm 1.09)\ \text{kJ mol}^{-1}/RT]$ cm^3 molecule^{-1} s^{-1}. Such behavior is explained by vibrationally excited N_2O enhancing the reaction at high temperatures. This rate coefficient expression, and the chemiluminescence cross section obtained in a previous study of the title reaction in a beam-scattering experiment, are used to estimate a photon yield of 12.5%. This yield is shown to be about half that predicted by a statistical consideration of the densities of states in the reactant electronic channels. In a separate experiment, the two-photon (193.3 nm) dissociation of CaO, produced by mixing a flow of Ca atoms and N_2O, is used to study the reaction $CaO + O \rightarrow Ca + O_2$, which proceeds at $(6.5 \pm 2.2) \times 10^{-10}$ cm^3 molecule^{-1} s^{-1} at 805 K.

Introduction

The reaction

$$Ca(^1S) + N_2O \rightarrow CaO + N_2 \qquad (1)$$

is one of a class of reactions of group 1 and 2 metals with N_2O that is of both theoretical and practical interest. These reactions tend to be highly exothermic, so that the metal oxide product is often formed in excited states giving rise to strong chemiluminescence. An important theoretical challenge has been to understand the branching ratios for the nascent production of the accessible product electronic states in these reactions, which involve multiple potential energy surfaces.[1,2] In the case of reaction 1, this chemiluminescent property has been studied extensively, both under single-collision conditions in molecular beams[3-7] and in diffusion flames.[8-13] A major practical interest in these types

(1) Alexander, M. H.; Dagdigian, P. J. *Chem. Phys.* **1978**, *33*, 13.
(2) Yarkony, D. R. *J. Chem. Phys.* **1983**, *78*, 6763.
(3) Irvin, J. A.; Dagdigian, P. J. *J. Chem. Phys.* **1981**, *74*, 6178.
(4) Dagdigian, P. J. *Chem. Phys. Lett.* **1978**, *55*, 239.
(5) Wang, J.; Menzinger, M. *Can. J. Chem.* **1983**, *61*, 2703.
(6) Jonah, C. D.; Zare, R. N.; Ottinger, Ch. *J. Chem. Phys.* **1972**, *56*, 263.
(7) Ottinger, Ch.; Zare, R. N. *Chem. Phys. Lett.* **1970**, *5*, 243.
(8) Bernard, D. J.; Slafer, W. D.; Lee, P. H. *Chem. Phys. Lett.* **1976**, *43*, 69.
(9) Capelle, G. A.; Jones, C. R.; Zorskie, J.; Broida, H. P. *J. Chem. Phys.* **1974**, *61*, 4777.
(10) Bernard, D. J.; Slafer, W. D.; Hecht, J. *J. Chem. Phys.* **1977**, *66*, 1012.

0022-3654/90/2094-5255$02.50/0

of reactions has been the development of infrared[14] and especially visible chemical lasers.[15-20]

Dagdigian and co-workers[3,4] and Zare and co-workers[6,7] have studied reaction 1 under single-collision conditions in Ca atom beam-scattering experiments. Irvin and Dagdigian[3] observed chemiluminescence from the $A^1\Sigma^+$, $A'^1\Pi$–$X^1\Sigma^+$ bands of CaO (600–890 nm), although this was very weak compared with the much more extensive emissions from the reactions of $Ca(^3P_J,^1D_2)$ with N_2O.[3-7] They reported a chemiluminescence cross section of 0.13 ± 0.07 Å^2 and estimated an upper limit to the total reaction cross section of 86 ± 5.5 Å^2, so that the photon yield was $\geq 0.15 \pm 0.09\%$. The collision energy of the atomic Ca beam in their study[3] corresponds to the average thermal collision energy at a temperature of 946 K. Kashireninov et al.[13] studied the kinetics of reaction 1 in a Ca–Ar–N_2O diffusion flame and obtained $k_1(T) = 2.7^{+0.3}_{-0.4} \times 10^{-11} \exp(-(23.4 \pm 10.0 \text{ kJ mol}^{-1})/RT)$ cm^3 molecule^{-1} s^{-1}. This result corresponds to a cross section of $0.14^{+0.33}_{-0.10}$ Å^2 at 946 K. Combining these results implies that the photon yield of reaction 1 is close to or greater than 100%, so that the studies do not appear to be consistent. Furthermore, the preexponential factor in the diffusion flame study[13] is rather small compared with recent temperature-dependent studies of other metal–N_2O reactions which have exhibited preexponential factors of the order of the collision number.[21-24] In fact, a similar inconsistency exists between the chemiluminescent cross sections of 4.8 ± 1.5 Å^2 for $Ca(^3P_J) + N_2O$ and 3.6 ± 1.9 Å^2 for $Ca(^1D_2) + N_2O$ from the study of Irvin and Dagdigian[3] and the total reaction cross sections of $0.36^{+1.08}_{-0.26}$ and $4.2^{+3.2}_{-1.9}$ Å^2, respectively, measured in a time-resolved study by Husain and Roberts.[25]

Reaction 1 has not been studied previously by a direct technique, and this will be the major objective of the present study. The thermal rate coefficients will be determined over a substantial range of temperature (250–900 K). There are two important theoretical reasons for this. Firstly, this reaction is a good candidate for investigating the role of reagent vibration in enhancing reaction rates.[23,26] In this instance, the effect on the thermal rate coefficients of vibrational excitation of N_2O in its low-frequency bending modes (588 cm^{-1} [27]) will be explored. Secondly, by assuming a Maxwell–Boltzmann distribution of reactant energies, the total reaction cross section will be estimated. This will then be used to investigate the current inconsistency between the chemiluminescence[3] and total reaction[13] cross sections noted above and lead to an accurate chemiluminescence photon (or quantum) yield for reaction 1.

An important application for the present study is to understand the chemistry of calcium in the mesosphere, where a layer of atomic Ca a few kilometers wide has been observed at an altitude of about 90 km.[28] The source of this Ca layer is believed to be meteoritic.[29] An interesting observation is that the ratio of the column densities of atomic Na to atomic Ca in the mesosphere is about 120:1,[28] although the metals have similar abundances in chondritic meteorites.[29] By analogy with atmospheric models of Na,[30] CaO is probably an initial sink for ablated Ca following reaction with O_3, and its greater bond energy compared to that of NaO[31] may render it less prone to reduction by atomic O:

$$CaO + O \rightarrow Ca + O_2 \qquad (2)$$

CaO is also thought to be an important intermediate in the oxidation of Ca seeded into a flame and to play a central role in the catalytic recombination of major flame radicals such as H and OH.[32,33] A further reason for studying reaction 1 is therefore to establish this reaction as a clean and efficient source of CaO. We will then proceed to investigate reaction 2, which does not appear to have been studied previously. During the course of this second study, information on the photodissociation of CaO at the ArF excimer wavelength (193.3 nm) was obtained, which will also be presented.

Experimental Section

Reaction 1 was investigated by the technique of time-resolved laser-induced fluorescence (LIF) spectroscopy of Ca atoms following the pulsed photolysis of CaI_2 vapor in an excess of N_2O and He bath gas. The experimental system has been described in detail elsewhere.[23] Briefly, the reaction was studied in a stainless steel reactor consisting of a central cylindrical reaction chamber at the intersection of two sets of horizontal arms which cross orthogonally. These arms provide the optical coupling of the lasers to the central chamber where the reaction was initiated, as well as the means by which the flows of N_2O and He enter the chamber. One of these arms is independently heated to act as a heat pipe source of CaI_2 vapor. The central chamber is enclosed in a furnace which can heat it to over 1100 K. Alternatively, the furnace can be filled with powdered solid CO_2 to cool the chamber to below 250 K. A fifth vertical side arm provides the coupling for the photomultiplier tube (PMT; Thorn EMI Gencom Inc., Model 9816QB) which monitors the LIF signal.

Powdered CaI_2 was placed in a tantalum boat in the heat pipe and then heated to about 940 K, where the concentration of the CaI_2 vapor in equilibrium above the molten salt is 2.9×10^{12} cm^{-3}.[31] The vapor was then entrained in a flow of He and carried into the central chamber. Although there was a major loss of CaI_2 vapor through deposition onto the relatively cool chamber walls, sufficient salt vapor reached the center of the chamber where it was photolyzed with an ArF excimer laser (Questek, Model 2110). The excimer beam was shaped by a system of lenses and a pinhole and then focused into the reactor.

The resulting $Ca(^1S)$ atoms were probed at $\lambda = 422.7$ nm ($Ca(4^1P_1)$–$Ca(^1S)$) with a nitrogen-pumped dye laser (Laser Science Inc., Model VSL-337; laser dye Stilbene 420, bandwidth ≈ 0.01 nm). In these experiments the excimer and dye lasers were arranged to be collinear and counterpropagating, with the dye laser protected from the excimer beam by a dichroic filter (Newport Corp., Model 10QM20HL1, wavelength cut-on at 400 nm). The diameter of the dye laser was carefully maintained to be $\approx 80\%$ that of the excimer by means of a beam expander. Resonant LIF was recorded with a gated integrator (Stanford Research Systems, Model SR250) after passing through an interference filter centered at 420 nm (Oriel Corp., fwhm = 10 nm).

Reaction 2 was studied by the pulsed photolysis of a mixture of CaO and N_2O in He bath gas. Ca metal was placed in the heat pipe and then heated to 908 K, where the concentration of Ca vapor is 2.51×10^{14} cm^{-3}.[31] The temperature of the heat pipe was maintained to within ± 1 K, monitored by an internal thermocouple in contact with the Ca metal. The Ca vapor was entrained in a flow of He and carried into the central chamber where it was mixed with a flow of N_2O/He to produce CaO through

(11) Eckstrom, D. J.; Barker, J. R.; Hawley, J. G.; Reilly, J. P. *Appl. Opt.* **1977**, *16*, 2102.
(12) Bernard, D. J.; Slafer, W. D.; Love, P. J.; Lee, P. H. *Appl. Opt.* **1977**, *16*, 2108.
(13) Kashireninov, O. E.; Kuznetsov, V. A.; Manelis, G. B. *Zh. Fiz. Khim.* **1977**, *51*, 958; *Russ. J. Phys. Chem. (Engl. Transl.)* **1977**, *51*, 566.
(14) Fenimore, C. P.; Kelso, J. R. *J. Am. Chem. Soc.* **1950**, *72*, 5045.
(15) Wren, D. J.; Menzinger, M. *J. Chem. Phys.* **1975**, *63*, 4557; *Discuss. Faraday Soc.* **1979**, *67*, 97.
(16) Wiesenfeld, J. R.; Yuen, M. J. *Chem. Phys. Lett.* **1976**, *42*, 293.
(17) Bourguignon, B.; Rostas, J.; Taieb, G. *J. Chem. Phys.* **1982**, *77*, 2979.
(18) Breckenridge, W. H.; Umemoto, H. *J. Phys. Chem.* **1983**, *87*, 1804.
(19) Cox, J. W.; Dagdigian, P. A. *J. Phys. Chem.* **1982**, *86*, 3738.
(20) Raiche, G. A.; Belbruno, J. J. *Chem. Phys. Lett.* **1987**, *134*, 341.
(21) Husain, D.; Marshall, P. *Combust. Flame* **1985**, *60*, 81.
(22) Husain, D.; Lee, Y. H. *Combust. Flame* **1987**, *68*, 177.
(23) Plane, J. M. C. *J. Phys. Chem.* **1987**, *91*, 6552.
(24) Plane, J. M. C.; Rajasekahr, B. *J. Phys. Chem.* **1989**, *93*, 3135.
(25) Husain, D.; Roberts, G. *Chem. Phys.* **1986**, *109*, 393.
(26) Plane, J. M. C.; Rajasekhar, B.; Bartolotti, L. *J. Chem. Phys.*, **1989**, *91*, 6177.
(27) Herzberg, G. *Molecular Spectra and Molecular Structure II. Infrared and Raman Spectra of Polyatomic Molecules*; Van Nostrand Reinhold: New York, 1945.
(28) Granier, C.; Jegou, J. P.; Megie, G. *Geophys. Res. Lett.* **1985**, *12*, 655.
(29) Goldberg, R. A.; Aikin, A. C. *Science* **1973**, *180*, 294.
(30) Swider, W. *J. Geophys. Res.* **1987**, *92*, 5621.
(31) *JANAF Thermochemical Tables*, 3rd ed.; Chase, Jr., M. W., Davies, C. A., Downey, Jr., J. R., Frurip, D. J., McDonald, R. A., Syverud, A. N., Eds.; *J. Phys. Chem. Ref. Data* **1985**, *14*.
(32) Cotton, D. H.; Jenkins, D. R. *Trans. Faraday Soc.* **1971**, *67*, 730.
(33) Jensen, D. E.; Jones, G. A. *Proc. R. Soc. London* **1978**, *A364*, 509.

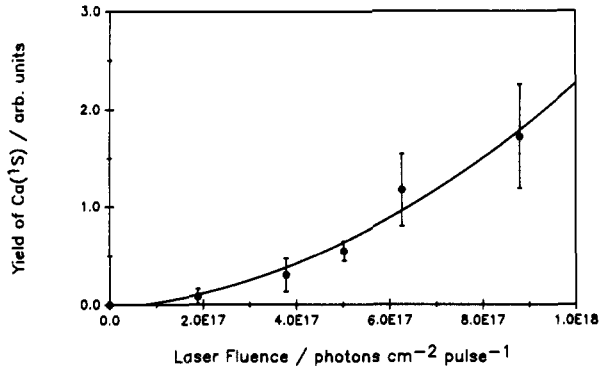

Figure 1. Plot of the yield of Ca(^{1}S) atoms, measured by LIF at 422.7 nm [Ca(^{1}P$_1$)–Ca(^{1}S)], as a function of the estimated excimer laser fluence at 193.3 nm employed in the pulsed photolysis of CaI_2 vapor in He bath gas.

reaction 1. The Ca atom concentration in the central chamber should be equal to the vapor concentration in the heat pipe, diluted by the ratio of the He mass flow through the heat pipe to the total of the mass flows mixing in the central chamber. We demonstrated that this was indeed the case (within 12%) by titrating the Ca in the central chamber, monitored by LIF, until sufficient N_2O was added to decrease the LIF signal to below the detection limit. During the kinetic studies, the added N_2O was in excess over the Ca concentration in the central chamber by a factor of between 2 and 20. Short turnover (residence) times, usually of less than 100 ms, of the gas mixture in the central chamber were employed in order to minimize the loss of CaO due to condensation on the reactor walls or cluster formation in the gas phase.

O atoms were then produced by photolyzing a small fraction of both the CaO and excess N_2O, using the ArF laser. Reaction 2 was monitored by the growth of the atomic Ca LIF signal, followed at longer reaction times by the loss of Ca due to reaction 1 with the excess N_2O.

Materials. Helium (99.9999%, Matheson, "Matheson Purity") was used without further purification. N_2O (99.99% pure, Matheson, Ultra High Purity) was degassed at 77 K before use. CaI_2 (99%+, Aldrich, Anhydrous) was refluxed in the heat pipe at 700–850 K for several hours prior to kinetic experiments to remove traces of I_2. Ca metal chips (Aldrich, 99%) were heated in the heat pipe at 900 K for about an hour prior to kinetic experiments.

Results

Ca + N_2O. Figure 1 illustrates the yield of Ca(^{1}S) atoms from the photolysis of CaI_2 vapor in He bath gas, plotted as a function of the estimated ArF laser fluence. The approximately quadratic relationship indicates that at least a two-photon process is occurring. This is in accord with an enthalpy change for the dissociation process

$$CaI_2 \rightarrow Ca(^1S) + 2I \qquad (3)$$

of ΔH_0° = 647 kJ mol^{-1},[31] for which one photon at 193.3 nm is not sufficiently energetic.

Under the conditions of the present study, in which the concentration of N_2O was always well in excess of the concentration of Ca atoms resulting from the pulsed photolysis of CaI_2 vapor, the loss of Ca atoms should be described by the pseudo-first-order decay coefficient, k', where

$$k' = k_{diff} + k_1[N_2O] \qquad (4)$$

The term k_{diff} describes diffusion of the Ca atoms out of the volume defined by the dye laser beam and within the field of view of the PMT.[23] Over the temperature range studied, the observed decays of the LIF signal were of a simple exponential form, $A \exp(-k't)$, if the ArF laser fluence through the center of the reactor was less than ca. 10^{17} photons cm^{-2} pulse^{-1}. An example of such a decay is shown in the main panel of Figure 2, illustrating the excellent signal-to-noise ratio obtained even at a reactor temperature as low as 286 K. However, at higher excimer laser fluences, the

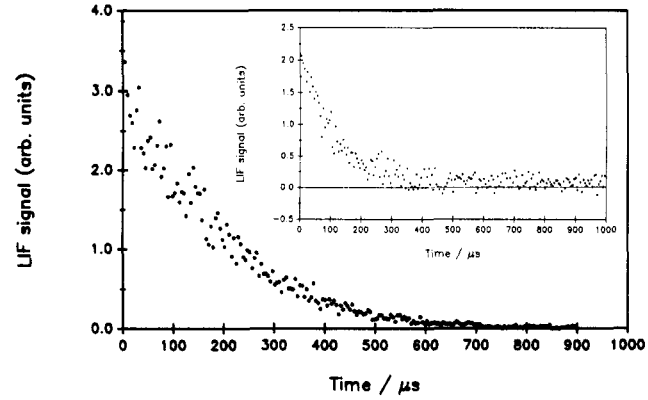

Figure 2. Time-resolved decays of Ca(^{1}S) atoms in an excess of N_2O and He, monitored by LIF at 422.7 nm [Ca(^{1}P$_1$)–Ca(^{1}S)] and formed by the pulsed laser photolysis at 193.3 nm of CaI_2 vapor. Main panel: reactor temperature = 286 K; [N_2O] = 1.43 × 10^{15} cm^{-3}; [He] = 6.9 × 10^{17} cm^{-3}; laser fluence ≈ 2 × 10^{16} photons cm^{-2} pulse^{-1}. Inset: 382 K, [N_2O] = 1.46 × 10^{15} cm^{-3}; [He] = 5.2 × 10^{17} cm^{-3}; laser fluence ≈ 6 × 10^{17} photons cm^{-2} pulse^{-1}.

decays became nonexponential. The inset in Figure 2 illustrates this effect: there is an initial rapid loss of Ca followed by a persistent tail of the Ca decay over a much longer time scale. This is most likely because the concentration of O atoms, resulting from the photolysis of N_2O, was sufficiently high to maintain a steady state between Ca and CaO through reactions 1 and 2, and the remaining few percent of Ca atoms were then removed by diffusion on a millisecond time scale. The photolysis of N_2O at 193.3 nm produces exclusively O(^{1}D) atoms,[34] which are then quenched by N_2O at essentially every collision:[35]

$$O(^1D) + N_2O \rightarrow 2NO \qquad (5a)$$

$$\rightarrow O_2 + N_2 \qquad (5b)$$

$$\rightarrow O(^3P) + N_2O \qquad (5c)$$

Thus, for the conditions of Figure 2, the O(^{1}D) will be removed with a half-life of ca. 2 μs. Taking the published photolysis cross section of N_2O at 193 nm[34] and our measured k_1 and k_2 (see below) indicates that physical quenching to O(^{3}P) (reaction 5c) accounts for <4% of reaction 5.

When the dependence of k' on [N_2O] was studied, the bath gas pressure was kept constant and in excess compared to that of N_2O, so that k_{diff} appeared as an intercept on a plot of k' against [N_2O]. The values of k_{diff}, measured in the absence of N_2O, ranged from ≈900 to 6000 s^{-1}. k_{diff} was shown to be inversely proportional to the total pressure of He in the reactor at constant temperature, and the values of k_{diff} were in accord with first-order loss of Ca atoms by diffusion out of the cylindrical volume of the dye laser beam.[23] This implied the absence of significant kinetic interferences from the use of CaI_2 as a precursor. Because the excimer laser beam was focused to a diameter of only 2–5 mm in order to achieve sufficient fluence for the multiphoton photolysis of CaI_2, and the dye laser beam diameter was maintained at ≈80% of that diameter, the Ca atoms diffused out of a relatively small volume, and these values of k_{diff} are somewhat higher than were observed previously when an unfocused flash lamp was used.[23,24] Because of the range of k_{diff} at different pressures and laser beam diameters, plots of $k'-k_{diff}$ vs [N_2O] are illustrated in Figure 3 for a selection of the temperatures at which reaction 1 was studied. k' exhibits a clear linear dependence on [N_2O]. The slopes of these plots thus yield k_1 as a function of temperature, listed in Table I.

We demonstrated that $k_1(T)$ was not a function of the bath gas pressure: such a dependence, especially at temperatures below 400 K, would imply that complex formation between Ca and N_2O was occurring, as was observed recently for the reaction Al +

(34) Okabe, H. *Photochemistry of Small Molecules*; Wiley: New York, 1978.

(35) Heidner, R. F.; Husain, D. *Int. J. Chem. Kinet.* **1973**, *5*, 819.

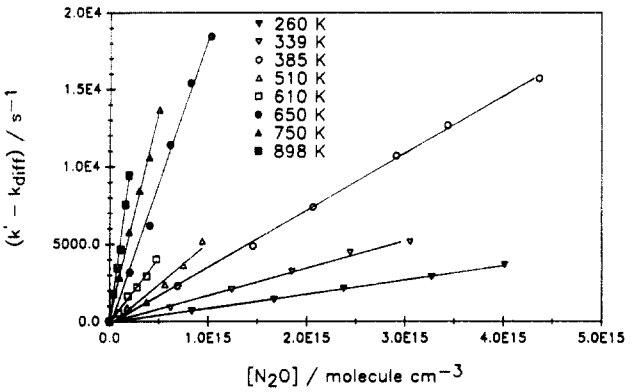

Figure 3. Plots of the pseudo-first-order rate coefficient k' with diffusional component k_{diff} subtracted, against $[N_2O]$ from 260 to 898 K. [He] ranged from (1–8) × 10^{17} cm^{-3}. Solid lines are linear regression curves through the data at each temperature.

TABLE I: Experimental Determinations of k_1(Ca+N_2O) as a Function of T^a

T/K	$k_1/10^{-12}$ cm^3 $molecule^{-1}$ s^{-1}	T/K	$k_1/10^{-12}$ cm^3 $molecule^{-1}$ s^{-1}
250	0.92 ± 0.04	533	8.56 ± 0.31
273	1.16 ± 0.04	610	17.4 ± 0.6
285	1.41 ± 0.02	650	18.7 ± 0.8
340	1.76 ± 0.06	750	26.8 ± 0.6
385	3.67 ± 0.06	850	38.7 ± 0.8
474	5.27 ± 0.21	898	48.1 ± 2.0
510	5.37 ± 0.51		

[a] Quoted uncertainty is 2σ.

CO_2.[36] When the temperature of the reactor was above 830 K, we observed that k_1 depended upon the turnover time of the gas mixture in the central chamber of the reactor: k_1 *increased* by about 20% when the turnover time was decreased from 1.2 to 0.6 s and then remained constant at shorter turnover times. We believe that this observation is accounted for by the heterogeneous loss of N_2O on the hot reactor walls,[23] which is not significant so long as the residence time in the reactor is relatively short. Nevertheless, at temperatures above 900 K, the heterogeneous loss of N_2O became too rapid to accommodate with the present reactor design, so that this temperature is the upper limit in the present study.

Figure 4 is an Arrhenius plot of the data contained in Table I and shows clear upward curvature at temperatures above 500 K. We fitted the data to two expressions commonly used to describe non-Arrhenius behavior, by means of a nonlinear least-squares fitting routine employing Marquardt's method.[37] The first, where $k(T) = AT^n \exp(-B/T)$, may be justified in terms of transition-state theory.[38,39] The best fit ($\chi^2 = 408.5$) to the present data yields, including standard errors

$$k_1(T) = (7.77 \pm 5.32) \times 10^{-17} T^{2.0\pm0.1} \exp[-(3.67 \pm 0.34 \text{ kJ mol}^{-1})/RT] \quad (6)$$

The value of n is determined by the difference between the heat capacities of the reagents and that of the transition state.[38] For the case of a reaction between an atom and a linear triatomic, $0.5 < n < 1.5$ for a collinear collision and $0.5 < n < 1.0$ for a bent transition state. The upper limits increase to 2.2 or 1.3, respectively, if anharmonicity is allowed in each vibrational mode.[38] Thus, the value of n in eq 6 is rather high, requiring a maximum contribution from the new vibrational degrees of freedom in the transition state, as well as a linear transition state.[38] Figure 4 illustrates the fit of eq 6 to the data. The data were also fitted

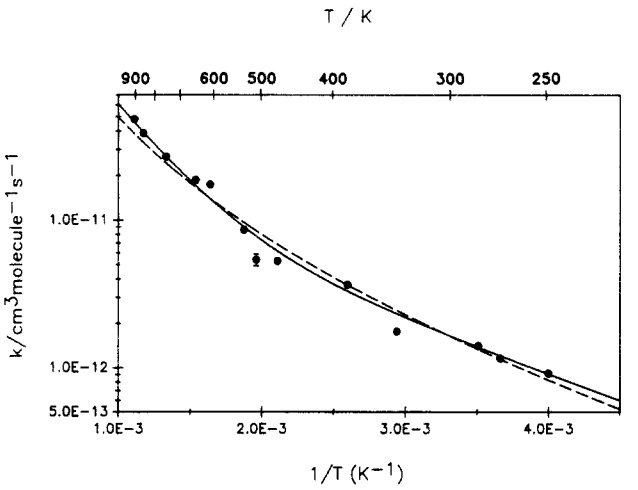

Figure 4. Arrhenius plot (ln (k_1) against $1/T$) over the temperature range 200–1000 K. The broken line is a best fit through the experimental data to the functional form $AT^{-n} \exp(-B/T)$; the solid line is a best fit to the form $A \exp(-B/T) + C \exp(-D/T)$.

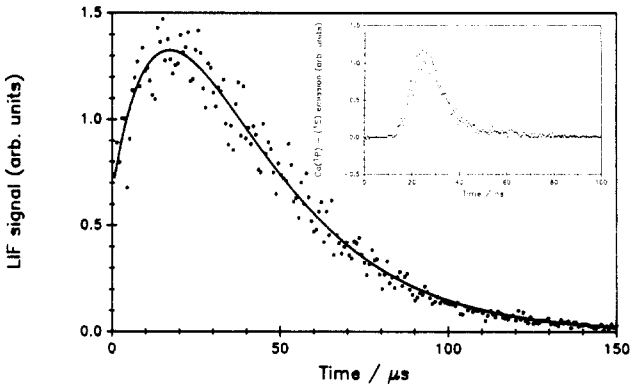

Figure 5. Main panel: time-resolved variation of the LIF signal at 422.7 nm [$Ca(^1P_1)$–$Ca(^1S)$], following the pulsed photolysis of CaO/N_2O in He at 193.3 nm; reactor temperature = 805 K; $[N_2O] = 1.1 \times 10^{15}$ cm^{-3}; $[CaO] = 1.3 \times 10^{14}$ cm^{-3}; $[He] = 6.1 \times 10^{16}$ cm^{-3}. The solid line through the experimental data is a fit using eq A5. Inset: time-resolved emission from $Ca(^1P)$–$Ca(^1S)$ at 422.7 nm, during the photolysis of CaO; [CaO] = 1.3×10^{14} cm^{-3}; excimer laser fluence ≈ 2×10^{17} photons cm^{-2} $pulse^{-1}$.

by the expression $k(T) = A \exp(-B/T) + C \exp(-D/T)$, which can be physically interpreted to imply that the reaction proceeds by two channels with different Arrhenius parameters.[23,40] The best fit ($\chi^2 = 220.6$) to the present data yields, including standard errors

$$k(T) = (2.43 \pm 0.29) \times 10^{-11} \exp[-(6.84 \pm 0.27) \text{ kJ mol}^{-1}/RT] + (9.70 \pm 1.39) \times 10^{-10} \exp[-(24.58 \pm 1.09) \text{ kJ mol}^{-1}/RT] \quad cm^3 \text{ molecule}^{-1} \text{ s}^{-1} \quad (7)$$

The fit of this functional form to the experimental data is also shown in Figure 4. An F test indicates that over the whole temperature range eq 7 is not a better fit than eq 6 at the 5% point of significance. Nevertheless, eq 7 is preferred because of the better fit at high temperatures, the unusually large value of n that is required in eq 6, and the form of eq 7 which expresses the low- and high-temperature dependences of reaction 1 as separate terms.

The Photolysis of CaO and the Reaction CaO + O. The main panel of Figure 5 illustrates the time-resolved production and loss of atomic Ca, monitored by LIF at 422.7 nm, following the pulsed 193.3-nm photolysis of CaO/N_2O in He bath gas. The photolysis of CaO was shown to be a multiphoton process. One of the photofragments is $Ca(^1P_1)$: the inset in Figure 5 illustrates the time-resolved emission at 422.7 nm ($Ca(^1P_1)$–$Ca(^1S)$) on a nanosecond time scale, from $Ca(^1P_1)$ formed during the excimer laser pulse. The initial delay of 15 ns before the appearance of the signal

(36) Parnis, J. M.; Mitchell, S. A.; Hackett, P. A. *Chem. Phys. Lett.* **1988**, *151*, 485.
(37) Press, W. H.; Flannery, B. P.; Teukolsky, S. A.; Vetterling, W. T. *Numerical Recipes: The Art of Scientific Computing*; Cambridge University Press: Cambridge, 1986; p 521.
(38) Cohen, N. *Int. J. Chem. Kinet.* **1989**, *21*, 909.
(39) Fontijn, A.; Zellner, R. In *Reactions of Small Transient Species*; Fontijn, A., Clyne M. A. A., Eds.; Academic: London, 1983.
(40) Fontijn, A.; Felder, W. *J. Chem. Phys.* **1977**, *67*, 1561.

is caused by the time of flight of the photoelectrons in the PMT. The emission decays exponentially with a lifetime of 8.3 ns. This is slightly longer than the lifetime of $Ca(^1P_1)$ of 4.6 ns,[41] because the longer duration of the excimer pulse (ca. 10–20 ns) obscured the faster spontaneous decay of $Ca(^1P)$. The peak height of the $Ca(^1P_1)$ emission was shown to be a function of the Ca flow from the heat pipe entering the reactor in an excess of N_2O and to be proportional to the N_2O concentration when the Ca vapor concentration was in excess. If spin multiplicity is conserved during the photodissociation process, the most likely products are

$$CaO(^1\Sigma^+) + 2h\nu\ (193.3\ nm) \rightarrow Ca(^1P_1) + O(^1D_2) \quad (8)$$

Reaction 8 requires a minimum energy of 870 kJ mol^{-1},[34,41,42] in accord with the observed two-photon yield of $Ca(^1P)$ emission during the excimer pulse or the yield of $Ca(^1S)$ observed by LIF about 1.2 μs after the excimer pulse. (The N_2-pumped dye laser has a 1.2-μs delay between being triggered and firing.) The $Ca(^1S)$ may all derive from $Ca(^1P)$ through reaction 8 or be formed directly. However, there was no evidence of $Ca(^1S)$ production from single-photon photolysis of CaO. Using a technique we have described previously,[43] we estimate the photodissociation cross section at 193.3 nm (one photon) to be less than 2×10^{-20} cm^2.

O atoms are also formed by the photolysis of both CaO and the excess N_2O in the reactor. As we have already discussed, $O(^1D_2)$ will be quenched very rapidly by the relatively large concentration of N_2O,[35] a small proportion being physically quenched to $O(^3P)$. Thus, in this experiment the Ca *and* O atoms are in a large excess of CaO and N_2O (see the caption to Figure 5), which greatly simplifies the kinetic analysis.

We fitted the time-resolved behavior of atomic Ca, exemplified in the main panel of Figure 5, by the analytical solution to the coupled differential equations describing the kinetics of Ca and O atoms in this system (see Appendix). There are two adjustable parameters in the fit: the $O(^3P)$ atom concentration formed by photolysis of CaO/N_2O and k_2. The initial $Ca(^1S)$ concentration is taken from the intercept of the LIF signal at $t = 0$, and k_1 is taken from the separate experiment described above (eq 7). The resulting fit, depicted by the solid line in Figure 5, is excellent. The ratio of $[O(^3P)]/[Ca(^1S)]$ formed by the flash is 18.5 ± 3.1, so that most of the $O(^3P)$ is derived from the photolysis of N_2O, as expected. The very good fit to the decay of Ca after 50 μs confirms that the value of k_1 extracted from the first set of experiments is correct. In order to observe a reasonable degree of atomic Ca growth by reaction 2, these experiments were performed with the maximum concentration of CaO obtainable with this reactor design: the heat pipe was run close to its maximum temperature, and a large mass flow of He was directed through the heat pipe. The central chamber was also kept at a high temperature to avoid any condensation of Ca on the walls of the heat pipe at the point where it is coupled to the reactor. A set of 15 such growth and decay curves were analyzed, where the N_2O concentration was varied by a factor of 10, yielding

$$k_2(805\ K) = (6.5 \pm 2.2) \times 10^{-10}\ \ cm^3\ molecule^{-1}\ s^{-1} \quad (9)$$

The possible role of the formation of clusters of the type Ca_xO_y should also be considered in this experiment. For instance, such clusters could provide a further photolytic source of Ca atoms. However, the value of k_2, which was calculated assuming all Ca flowing into the reactor was converted to gas-phase CaO only, is essentially at the collision number. Hence, only a very limited loss of CaO could have occurred through clustering (or wall loss).

Discussion

$Ca(^1S) + N_2O$. Reaction 1 exhibits substantial non-Arrhenius behavior. Although eq 7 is primarily an analytical fit to the data, we have shown previously[23] that the two Arrhenius-type terms may contain interesting physical information. By analogy with the ab initio study of Yarkony[2] on the potential surface of $Mg(^1S) + N_2O$, reaction 1 is expected to be favored by collinear attack of the Ca atom on the oxygen end of N_2O, leading to a charge transfer from the Ca to the lowest unoccupied 3π (10a) orbital of N_2O, forming the initially linear ($^2\Pi$) state of N_2O^-.[44] This charge transfer is the crucial step for successful reaction; because of the small electron affinity of N_2O (0.39 eV[2]) and the relatively large ionization energy of $Ca(^1S)$ (6.11 eV[41]), this reaction cannot proceed by an electron capture or "harpoon" mechanism.[23,45,46]

In fact, in a collinear collision there will be very poor spatial overlap between the Ca 4s orbital and the 3π orbital of N_2O, so that the probability of a charge transfer will be very small. However, a mixing of the $Ca(^1S)$ with the excited $^1D_2$ or $^1P_1$ states will increase the orbital overlap between the reactants and hence facilitate the charge transfer. Figure 6 consists of a pair of diagrams showing the correlations between the reactant and product states through the ionic intermediates. Note that if the ionic intermediates in Figure 6 actually formed stable charge-transfer complexes, these would also correlate with the $a^3\Pi_i$ and $b^3\Sigma^+$ triplet states of CaO. However, assuming that reaction 1 is concerted, only singlet products are likely to be formed. Under $C_{\infty h}$ symmetry, Figure 6a, the $Ca^+(^2S)\cdot N_2O^-(^2\Pi)$ intermediate correlates with $Ca(^1D_2) + N_2O$, *not* with the ground-state reactants. However, under C_s symmetry the situation illustrated in the correlation diagram in Figure 6b will obtain, especially if the collisions are nearly collinear. The $^1A'$ surface of the incoming reactants will undergo an avoided crossing with the $^1A'$ surface arising from $Ca(^1D_2) + N_2O$ and then undergo a second avoided crossing between the ionic intermediates and the products.

A completely adiabatic reaction under C_s symmetry will thus proceed along the lowest $^1A'$ adiabatic surface. However, there

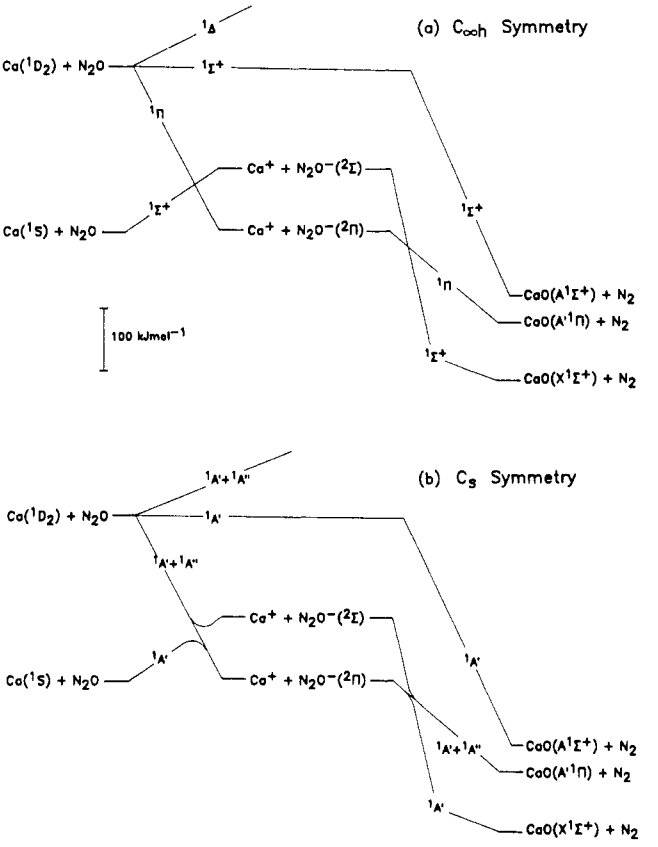

Figure 6. Adiabatic correlation diagrams under $C_{\infty h}$ and C_s symmetry of the reaction between Ca and N_2O, involving an intermediate charge-transfer complex. The relative energies of the reactants and the products are shown to scale.

(41) *Handbook of Physics and Chemistry*, 65th ed.; Weast, R. C., Ed.; CRC Press: Boca Raton, FL, 1985.
(42) Irvin, L. A.; Dagdigian, P. J. *J. Chem. Phys.* **1980**, *73*, 176.
(43) Rajasekhar, B.; Plane, J. M. C.; Bartolotti, L. *J. Phys. Chem.* **1989**, *93*, 7399.
(44) Bardsley, J. N. *J. Chem. Phys.* **1969**, *51*, 3384.
(45) Levy, M. *J. Phys. Chem.* **1989**, *93*, 5195.
(46) Jalink, H.; Harren, F.; Van den Ende, D.; Stolte, S. *Chem. Phys.* **1986**, *108*, 391.

will be a barrier to charge transfer in the entrance channel, as shown in Figure 6b. The energetic accessibility of the excited open-shell $Ca(^1D_2)$ (or $Ca(^1P_1)$) states will determine the height of this barrier at the crossing point between the reactants and the charged intermediates.[45] Yarkony[2] has pointed out that because the $Ca(^1D_2,^1P_1)$ states are much closer to the $Ca(^1S)$ ground state compared with Mg, reaction 1 is reactive whereas the analogous Mg reaction is extremely slow.

The barrier height in the entrance channel will thus be determined by the degree of collinearity of the reaction. However, even if the entrance channel for reaction 1 strongly favors collinear reaction, the $C_{\infty h}$ symmetry will be relaxed to C_s symmetry if the N_2O is vibrationally excited in its degenerate bending modes (ν_2). Thus, vibrational excitation will facilitate the charge transfer, turning on the reaction. Inspection of eq 7 shows that the first term, which describes the kinetic behavior of reaction 1 at temperatures below 500 K, is characterized by a small energy barrier and preexponential factor. The second term in eq 7, which describes the rate constant at high temperature, will then include the Boltzmann probability of the N_2O being vibrationally excited.[23]

As shown in Figure 6, the energetically and adiabatically accessible pathways for reaction 1 include[3,31,42]

$$Ca(^1S) + N_2O \rightarrow CaO(X^1\Sigma^+) + N_2 \qquad \Delta H_0 = -(235.7 \pm 6.8) \text{ kJ mol}^{-1} \quad (1a)$$

$$\rightarrow CaO(A'^1\Pi) + N_2 \qquad \Delta H_0 = -(132.8 \pm 6.8) \text{ kJ mol}^{-1} \quad (1b)$$

$$\rightarrow CaO(A^1\Sigma^+) + N_2 \qquad \Delta H_0 = -(97.6 \pm 6.8) \text{ kJ mol}^{-1} \quad (1c)$$

We can calculate the branching ratios into these allowed product electronic states by using the approach of Alexander and Dagdigian.[1] This is based on the total volume of translational phase space associated with each electronic channel. The total density of states corresponding to product channel α, summed over all internal vibration–rotation levels of $CaO(\alpha)$ and N_2, is given in the classical limit by[1]

$$\rho_\alpha(E_\alpha) \approx (4/15) \sum_{\nu 1 \nu 2} (B_{\nu 1} B_{\nu 2}^{\alpha})^{-1} (E_\alpha - G_{\nu 1} - G_{\nu 2}^{\alpha})^{5/2} \qquad (10)$$

where E_α is the total energy, excluding electronic excitation of CaO, in the product channel, B and G are rotational and vibrational constants with their usual meaning,[47] and the subscripts 1 and 2 refer to the products N_2 and CaO in electronic state α. The necessary spectroscopic information and energy levels of the product electronic channels of reaction 1 are given in refs 25 and 47. The statistical branching ratios are given by[1]

$$P^0_\alpha = g_\alpha \rho_\alpha(E_\alpha) / \sum_\alpha g_\alpha \rho_\alpha(E_\alpha) \qquad (11)$$

where g_α is the statistical weight factor of each electronic state CaO (g_α = 1, 2, and 1 for the X, A', and A states, respectively). Note that we have assumed spin conservation; hence, the energetically accessible $a^3\Pi$ and $b^3\Sigma^+$ states of CaO are not considered (see above). We have calculated the branching ratios into the three product states at collision and internal energies corresponding to temperatures of 300 and 946 K. This choice of temperatures is explained below. The branching ratios are listed in Table II, which illustrates that the branching into the excited states increases with greater reactant collision energy and the internal energy of N_2O.

The beam-scattering experiments of Irvin and Dagdigian[3] employed a Ca beam with a velocity of 1.06×10^5 cm s^{-1}, colliding with a low pressure of N_2O which we assume was thermally equilibrated at room temperature. The collision energy in this experiment[3] is equivalent to the average thermal collision energy at a temperature of 946 K, whereas the internal energy of the N_2O was presumably equivalent to a temperature of 300 K. In order to compare with our measurements of the total reaction cross section, only the low-temperature term in eq 7 should be used, in order to calculate the rate constant at 946 K *in the absence* of a significant population of $N_2O(\nu_2>0)$, yielding $k_1(946 \text{ K}) = (1.02 \pm 0.20) \times 10^{-11}$ cm^3 molecule^{-1} s^{-1}. Assuming the approximation

$$k(T) \approx \sigma(T)(8k_BT/\pi\mu)^{1/2} \qquad (12)$$

where $\sigma(T)$ is the reaction cross section, k_B is Boltzmann's constant, and μ is the reduced mass of the collision partners, yields $\sigma(946 \text{ K}) = 1.04 \pm 0.21$ Å^2. Combined with the chemiluminescent cross section[3] of 0.13 ± 0.07 Å^2, the photon yield of reaction 1 is then $12.5^{+11.6}_{7.7}$%. The final row in Table II shows the predicted branching ratios for the case of a collision temperature of 946 K and an internal temperature of 300 K. The calculated photon yield, i.e., fractional production of $CaO(A'\Pi$ and $A^1\Sigma^+)$, is 26.0%. This is roughly twice as large as the experimental photon yield derived above, which is to be expected since the statistical prediction does not take account of the degree of adiabaticity of the reaction and is thus an upper limit: a fully adiabatic reaction would have a zero photon yield.

TABLE II: Branching Ratios P_α^0 into the Product Electronic Channels $CaO(\alpha) + N_2$ of the Reaction Ca + N_2O, at Combinations of Translational and Internal Temperatures

		α		
T_{trans}[a]/K	T_{int}[b]/K	$X^1\Sigma^+$	$A'^1\Pi$	$A^1\Sigma^+$
300	300	0.76	0.22	0.02
946	946	0.70	0.28	0.02
946	300	0.74	0.24	0.02

[a] The translational impact energy is given by $1.5k_BT$, where k_B is Boltzmann's constant. [b] The internal energy is given by $k_BT + \sum h\nu_i/(\exp(h\nu_i/k_BT) - 1)$, where h is Planck's constant, ν_i are the vibrational frequencies of N_2O, and the summation is over all vibrational degrees of freedom.

The only previous studies of reaction 1 to compare with the present result are the beam-scattering experiment of Irvin and Dagdigian[3] and the diffusion flame study of Kashireninov et al.[13] The former workers[3] obtained an *upper limit* to the total reaction cross section of 86.6 ± 5.5 Å^2 and commented that this large cross section might have been due to a significant elastic scattering contribution to Ca loss in the beam. Comparison with our estimated cross section indicates that this probably was the case. The second group[13] obtained an activation energy over the temperature range 923–1073 K of 23.4 kJ mol^{-1}, in very good agreement with the activation energy we derived in the high-temperature Arrhenius term in eq 7. Unfortunately, the preexponential term in the diffusion flame study[13] is a factor of about 14 smaller than our measurement. We believe that in the diffusion flame study,[13] which necessarily relies on the extraction of a rate constant by modeling a complex system, the values of $k_1(T)$ obtained probably reflected a combination of elementary reactions of which reaction 1 has the largest temperature dependence. Thus, the correct temperature dependence but incorrect preexponential factor were obtained.

Finally, Husain and Roberts[25] reported temperature-dependent rate coefficients for the reactions $Ca(^3P_J)$ and $Ca(^1D_2)$ with N_2O, obtaining total reaction cross sections which are small compared with the chemiluminescent reactions from the beam study[3] (see Introduction). In their experiment,[25] Ca vapor was mixed with a flow of N_2O/He in a slow flow through a heated reactor. Ca atoms were pumped to the ^3P_J or $^1D_2$ states, and the subsequent reactions were monitored by emission from the forbidden transitions to the ^1S ground state. Our present work demonstrates that in such a system the Ca vapor and N_2O in the reactor would react together rapidly to produce CaO. Indeed, the experimental arrangement we employed to study reaction 2 at 805 K was similar to that used by Husain and Roberts,[25] except that in our system the Ca vapor was flowed into the reactor from a separately heated side arm rather than arising from heated Ca in the reactor itself. The fact that Husain and Roberts[25] were able to observe emission

(47) Herzberg, G. *Spectra of Diatomic Molecules*, 2nd ed.; Van Nostrand: Princeton, NJ, 1965.
(48) Smith, I. W. M. *Kinetics and Dynamics of Elementary Gas Reactions*; Butterworths: London, 1980.

from excited Ca atoms at temperatures between 725 and 900 K, where the N_2O concentration entering their reactor was in excess over the equilibrium Ca vapor pressure, suggests that most of the N_2O was removed in situ, possibly through a heterogeneous reaction with hot solid Ca. At temperatures between 900 and 1100 K, the Ca vapor pressure would have been in excess over the N_2O. Thus, the time-resolved molecular emission which those workers[25] observed from excited CaO was most likely the result of electronic energy transfer from $Ca(^3P_J,^1D_2)$ to CaO, and the measured rate constants for the quenching of these excited atomic states are for reaction with CaO rather than N_2O.

CaO + O. Although there is some uncertainty regarding the bond energy of CaO,[42] assuming the recent value[42] of $D_0(Ca-O) = 396.5 \pm 6.8$ kJ mol^{-1} indicates that reaction 2 is exothermic by about 101 kJ mol^{-1}. Equation 9 implies that reaction 2 proceeds at the collision number and hence possesses a negligible energy barrier. The temperature dependence of reaction 2 may thus be expressed as[48]

$$k_2(T) = (4.0 \pm 1.3) \times 10^{-10}(T/300)^{1/2} \text{ cm}^3 \text{ molecule}^{-1} \text{ s}^{-1} \quad (13)$$

Although this reaction has not been studied previously, we have observed a similar absence of an energy barrier for the analogous reaction NaO + O.[49]

Mesospheric Implications. We pointed out in the Introduction the atmospheric significance of studying reaction 2, namely, to understand the observed depletion of atomic Ca relative to atomic Na, in the mesosphere at about 90 km. The present result (eq 13) indicates that the reduction of CaO to Ca by atomic O is too rapid for CaO to be a significant reservoir for ablated Ca in the mesosphere. We are therefore proceeding to examine the chemistry of calcium superoxide, CaO_2, as a possible explanation for the low mesospheric abundance of atomic Ca.[28]

Acknowledgment. This work was supported under Grant ATM-8820225 from the National Science Foundation.

Appendix

The reaction CaO + O was studied by photolyzing CaO/N_2O under conditions of excess N_2O, such that the loss of Ca by reaction 1 was rapid and diffusional loss could be neglected. Thus

$$d[Ca]/dt = k_2[CaO][O] - k_1[Ca][N_2O] \quad (A1)$$

$$d[O]/dt = -k_2[CaO][O] \quad (A2)$$

Since both CaO and N_2O are in pseudo-first-order excess over Ca and O

$$d[Ca]/dt = k_2'[O] - k_1'[Ca] \quad (A3)$$

$$d[O]/dt = -k_2'[O] \quad (A4)$$

If $[Ca]_0$ and $[O]_0$ are the concentrations of these atoms formed by the photolysis of CaO and N_2O, and assuming effectively instantaneous quenching of $O(^1D)$ formed from the photolysis of N_2O (see text), then the atomic Ca concentration at time t is given by

$$[Ca] = ([Ca]_0 + k_2'/(k_2' - k_1')[O]_0)\exp(-k_1't) - k_2'/(k_2' - k_1')[O]_0 \exp(-(k_2' - 2k_1')t) \quad (A5)$$

(49) Plane, J. M. C.; Husain, D. *J. Chem. Soc., Faraday Trans. 2* **1986**, *82*, 2047.

Kinetics of the Reaction OH + NH_3 in the Range 273–433 K

Eric Wei-Guang Diau, Tai-Ly Tso, and Yuan-Pern Lee*,†

Department of Chemistry, National Tsing Hua University, 101, Sec. 2, Kuang Fu Road, Hsinchu, Taiwan 30043, R.O.C. *(Received: December 4, 1989; In Final Form: February 21, 1990)*

The kinetics of the reaction OH + NH_3 have been studied by means of the flash photolysis/laser-induced fluorescence technique. The rate of this reaction was investigated in the range 273–433 K under more extensive conditions ($68 < P/\text{Torr} < 504$, $0.29 < [NH_3]/10^{15}$ molecules cm^{-3} < 36.1) than previously. The results from experiments with the Xe lamp and with the KrF laser for photolysis agree well within the experimental uncertainties, indicating the absence of interference due to excess NH_2 which was produced by photolysis with the Xe lamp. A fit of rate coefficients to the Arrhenius equation yields $k = (3.29 \pm 1.02) \times 10^{-12} \exp[-(922 \pm 100)/T]$ cm^3 molecule^{-1} s^{-1}, with $k = (1.47 \pm 0.07) \times 10^{-13}$ cm^3 molecule^{-1} s^{-1} at 297 K; the uncertainties represent one standard error. The rate constant of the interfering reaction, OH + NH_2 → products, was also estimated to be less than 7×10^{-12} cm^3 molecule^{-1} s^{-1}.

Introduction

Although ammonia is a minor constituent of the terrestrial atmosphere, it plays a significant role in both homogeneous and heterogeneous atmospheric reactions.[1,2] Being the dominant basic gas in the atmosphere, ammonia partially neutralizes atmospheric acids in precipitation. On the other hand, NH_3 may be oxidized in the atmosphere to odd-nitrogen species which contribute to the acidity of precipitation.

The rate-determining step in the oxidation of NH_3 is its reaction with hydroxyl radical:

$$OH + NH_3 \rightarrow H_2O + NH_2 \quad (1)$$

The ultimate fate of amidogen radical (NH_2) formed in reaction 1 is not well understood. NH_2 could be a significant source of atmospheric NO_x by its reaction with O_2 or O_3, otherwise a significant sink via the reactions of NH_2 with NO or NO_2. The rates and mechanisms of these potentially important reactions of NH_2 require further studies.[3,4] Similarly, reaction 1 is also important in the conversion of fuel nitrogen to NO_x[5] and in the removal of NO_x from fuel gases in combustion by the addition of NH_3.[6]

† Also affiliated with the Institute of Atomic and Molecular Sciences, Academia Sinica, R.O.C.

(1) McConnell, J. C. *J. Geophys. Res.* **1973**, *78*, 7812.
(2) Wofsy, S. C.; McElroy, M. B. *Can. J. Chem.* **1974**, *52*, 1582.
(3) DeMore, W. B.; Golden, D. M.; Hampson, R. F.; Howard, C. J.; Kurylo, M. J.; Molina, M. J.; Ravishankara, A. R.; Sander, S. P. *JPL Publ.* **1987**, *No. 87-41*.
(4) Westley, F.; Herron, J. T.; Cvetanovic, R. J.; Hampson, R. F.; Mallard, W. G. NIST Chemical Gas Kinetics Database, Ver. 1.1 (*NIST Stand. Ref. Database* **1989**, *17*).
(5) Song, Y. H.; Blair, D. W.; Siminski, V. J.; Bartok, W. *Symp. (Int.) Combust., [Proc.], 18th* **1981**, 53.

0022-3654/90/2094-5261$02.50/0